Article

Step-Climbing Tactics Using a Mobile Robot Pushing a Hand Cart

Hidetoshi Ikeda * , **Takuya Kawabe, Ryousuke Wada and Keisuke Sato**

National Institute of Technology, Toyama College, 13 Hongo-Chou, Toyama 939-8630, Japan;
toyama_nct_ikedah_lab@yahoo.co.jp (T.K.); ikedalabo.tnct@gmail.com (R.W.); sato@nc-toyama.ac.jp (K.S.)

* Correspondence: ikedah@nc-toyama.ac.jp; Tel.: +81-764-93-5444

check for updates

Abstract: The present paper describes step-climbing tactics using a wheeled robot and a hand cart that has a hand brake. The robot has two arms that are used to hold or push the handle of the cart and a lower extendable wheel mechanism that can push against the bottom of the cart. Some of the manipulator joints are controlled passively when moving over the step. To lift the front wheels of the cart, the robot holds the handle steady and pushes against the bottom of the cart using the extendable wheel mechanism. This action is similar to that performed by a human. The robot then pushes the entire cart forward so that the front wheels of the cart are above the step. When the rear wheels of the cart have climbed the step, the upper-arm links of the manipulators are pressed against the robot chest to allow the robot to push the cart. When the cart has fully climbed the step, the robot then uses the cart to climb the step. The present paper describes the details of the robot system, and theoretical analyses were performed to determine the requirement of masses and the centers of gravity of both vehicles to lift the cart. Experiments were also carried out in which the robot was controlled using an intranet connection, and the results demonstrated the effectiveness of the proposed method.

Keywords: cart; robot; step climbing; transportation; stopper

1. Introduction

Hand carts and shopping carts are used all over the world to help people convey baggage. In recent years, several robotic carts have been investigated, including an autonomous cart that follows the user [1,2], a robotic cart that helps the operator when transporting heavy baggage [3], and transportation using a cart connected to an omnidirectional mobile robot [4,5]. Iwanuma et al. studied two shopping assistant robots that can be used in supermarkets [6]. They proposed not only a cart robot, which has a shopping basket attached to the robot body for transportation of an item, but also a humanoid with dual manipulators, which can bring the shopping basket. If the partner robot can operate a cart freely, the possibilities of transportation using a cart for improvement are endless. Research on such carts that can be manipulated by a partner robot has been carried out. Ohno proposed a method of transportation of a hand cart using ASIMO (HONDA Co., Ltd., Tokyo, Japan), a legged locomotion robot with dual manipulators [7]. Similarly, Inaba et al. studied the locomotion of a wheelchair, rather than a cart, using a legged locomotion robot [8]. However, they showed how to push and transport a wheelchair using a personal robot with dual manipulators.

A hand cart has a wheel mechanism that it uses to move. Excellent energy efficiency is one of the advantages of a wheel mechanism. It is easy for people to move a hand cart on a flat road. However, it is difficult for a vehicle that has a wheel mechanism to move up and down steps. Numerous research programs aimed at improving the mobility of wheel mechanisms on steps have been conducted, based on the following strategies: additional legs [9,10], multiple wheels and variable wheelbases [11], and a combination of an adjustable center of gravity (COG) and multiple

wheels [12]. Reports of multiple vehicles cooperating for crossing irregular terrain include those of Asama et al. [13], who considered a forklift system. Transporting a cart using a mobile robot that has numerous manipulators, similar to the human arm, is not an easy task. When the cart is heavier than the robot, controlling a robot to push or pull the cart is very difficult because the reaction force from the cart strongly influences the robot. In particular, one weakness for a wheeled vehicle is step climbing [14]. In transporting heavy baggage using a push-cart, it is very difficult to control the cart at a step because the incline of the vehicle is always changing, and the reaction force from the cart is also changing. As such, there have been no studies of a cart climbing a step using a partner robot.

The research group of the present study has achieved cooperative step climbing using a wheelchair and a partner robot with manipulators [15] and have proposed a cooperative step-climbing system using a hand cart and a robot [16]. In the present paper, we intend to describe in detail the concept of step climbing of a hand cart and present the results of both theoretical analysis and experiments.

The proposed step-climbing method uses the difference in velocity between connected vehicles, which considers not only the robot driving force, but also the wheelchair driving force. However, since a typical hand cart does not generate a driving force, the step-climbing method that we have proposed for a wheelchair cannot be applied to a hand cart. The present paper proposes a step-climbing method for a hand cart and a partner robot that uses an action that is similar to that performed by a human.

Based on preliminary measurements of friction coefficients using the vehicles in wet and dry conditions on asphalt, concrete, wood, and interior flooring, the ground surface considered in the present study was assumed to have a friction coefficient in the range 0.6 to 0.9, which satisfies all of the above conditions. The heights of steps at the entrances of typical buildings and other structures were measured, and the target step height was set to 120 mm, which accounts for more than 80% of the observed heights.

The remainder of the present paper is organized as follows. Section 2 describes the step-climbing system using a robot and a hand cart. Section 3 describes the process of climbing a step. Section 4 provides a theoretical analysis. Section 5 presents the experimental results. Section 6 concludes the paper.

2. Hand Cart and Robot

This system consists of a wheeled robot and a hand cart (Figure 1). The robot used in the present study was the wheeled "Tateyama", which was developed in our laboratory. This robot has three sets of wheels (front, middle, and rear) paired on the left and right. The front pair of wheels are casters, and the middle and rear pairs of wheels are driving wheels. The rear pair of wheels can be shifted in position, and this mechanism is used by the robot to climb steps (Figure 2, see Section 3). The hand cart and robot are deployed in a forward-and-aft configuration (Figure 3). The specifications of the robot and the hand cart are shown in Tables A1 and A2 (Appendix A).
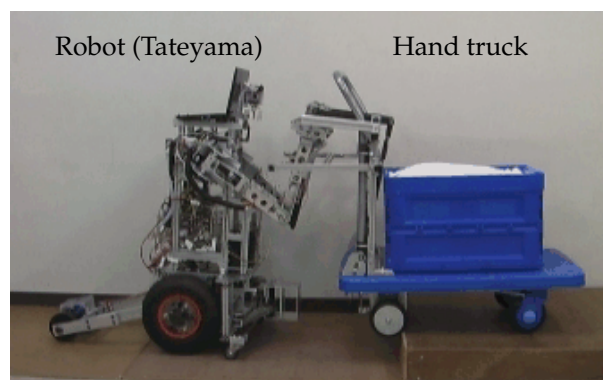

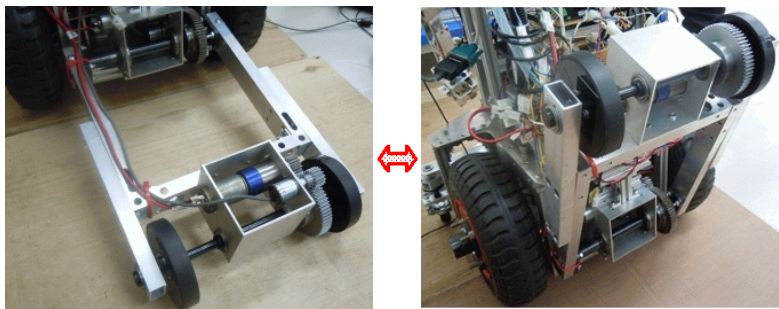**Figure 1.** Photograph of the robot and the hand cart.

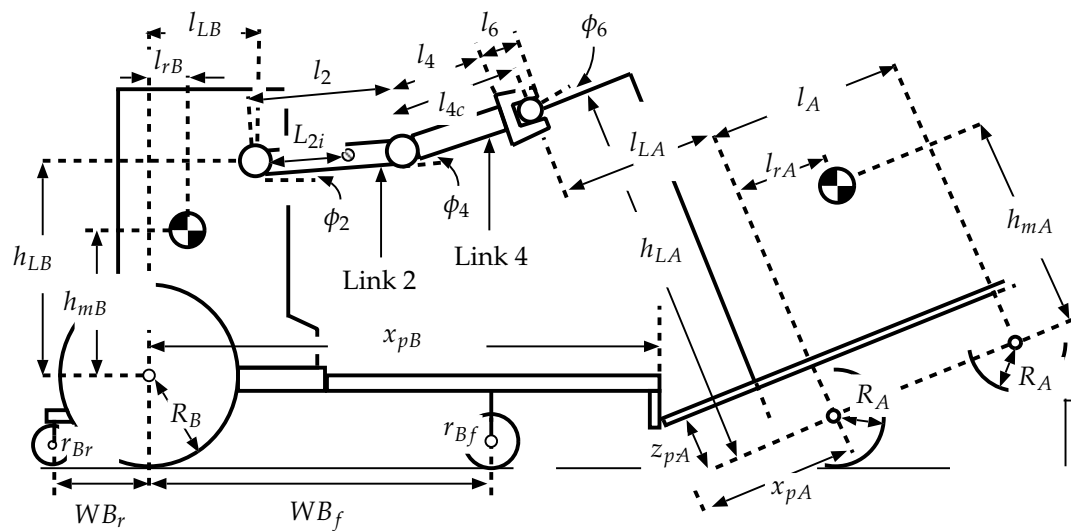**Figure 2.** Robot rear wheel mechanism.

Figure 3. Model of the robot and the hand cart.

Figure 4 shows the process in which a human moves a hand cart over a step. Most people push the rear bottom of the cart with their foot when lifting the front wheels of the hand cart during step climbing. When some people push and lift the rear wheels of a heavy cart, they limit the passive rotation about the shoulder joints as the upper arms are pushed into their chest. In the present paper, this motion is performed using the front-wheel mechanism of the robot (Figures 5 and 6) and the robot stopper (Figure 7).
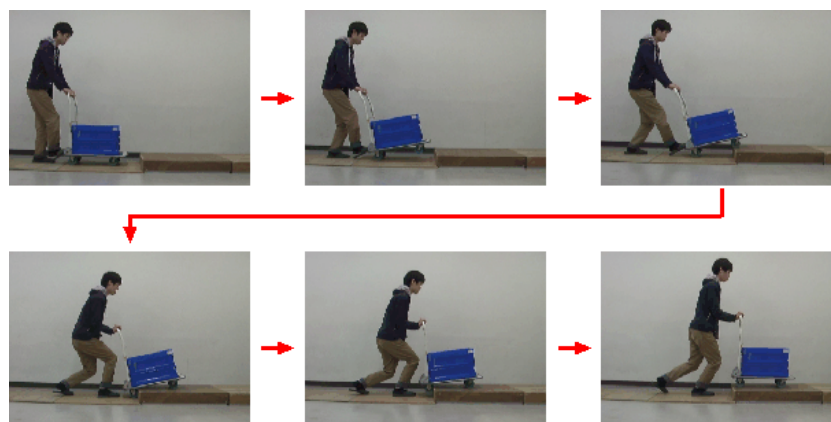

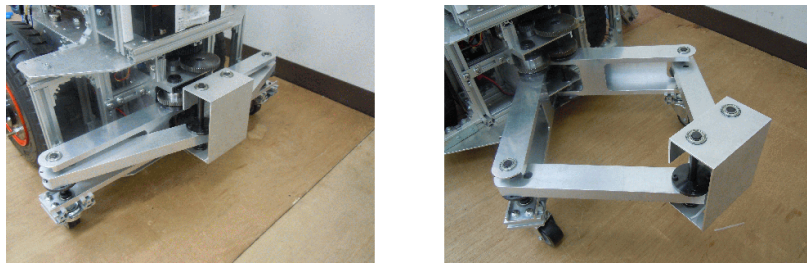**Figure 4.** Human method of pushing a hand cart up a step.

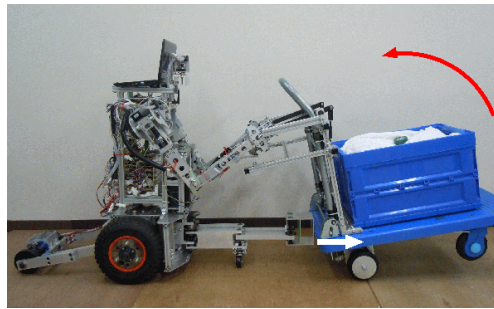**Figure 5.** Extendable robot front-wheel mechanism.

Figure 6. Robot pushing against the bottom of a hand cart using the front-wheel mechanism.
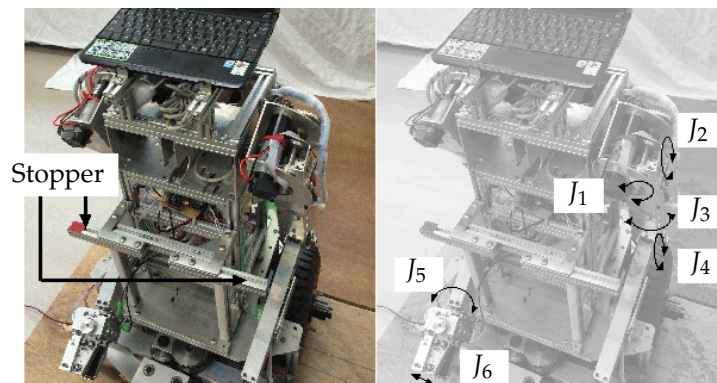

Figure 7. Stopper on the robot and manipulator joints.

The robot has manipulators attached to the left and right sides of its upper half. In addition to the five degrees of freedom (DOFs) of the arm, the hand has one DOF, for a total of six DOFs (Figure 7). The manipulator joint angles are -90 [deg] $\leq \phi_2 \leq +90$ [deg] and 0 [deg] $\leq \phi_4 \leq +100$ [deg]. The robot has a stopper mounted on the front of its body (Figure 7). First, the upper links of the manipulators are located behind the stopper when the front wheels of the cart are lifted (Figure 8). As described below (Section 3), the manipulators are pulled when lifting the front wheels of the cart so that the front-wheel mechanism of the robot can reach the rear bottom of the cart when lifting the front wheels of the cart.

The manipulators are pulled by the cart when the front wheels of the cart ascend the step, and the stopper limits the passive rotational travel around the shoulder axes of the manipulators (Figure 9, Section 3). After climbing of the front wheels of the cart, the upper links of the manipulators are located in the front of the stopper (Figure 10). When the rear wheels of the cart climb a step, the manipulators of the robot are pushed by the force from the cart. However, the stopper of the robot limits the passive rotational travel of the manipulator (Figure 10, Section 3). This enables the robot to imitate a human pushing an object by limiting the passive rotation about the shoulder joints as the upper arms are pushed into the chest (Figure 4).
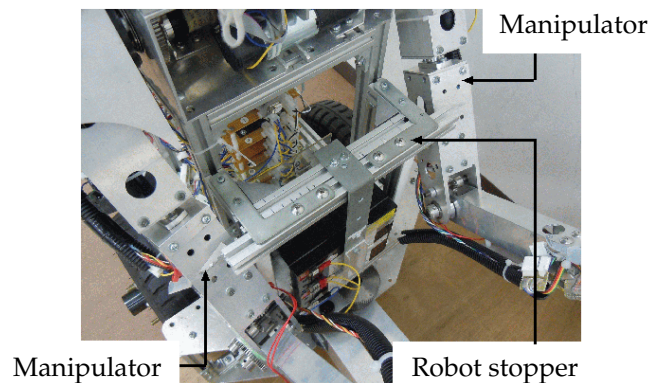
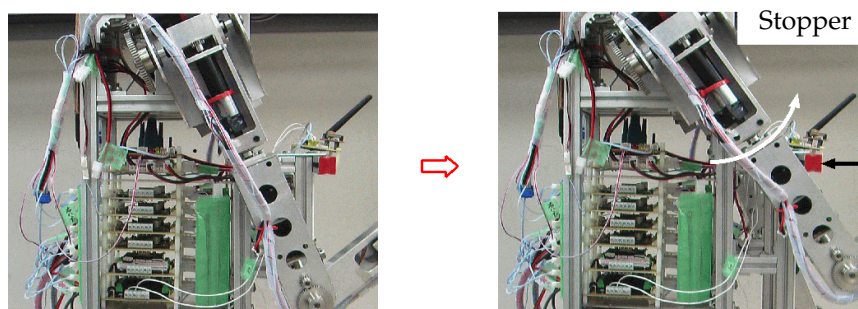**Figure 8.** Locations of manipulators for lifting the front wheels of the cart.

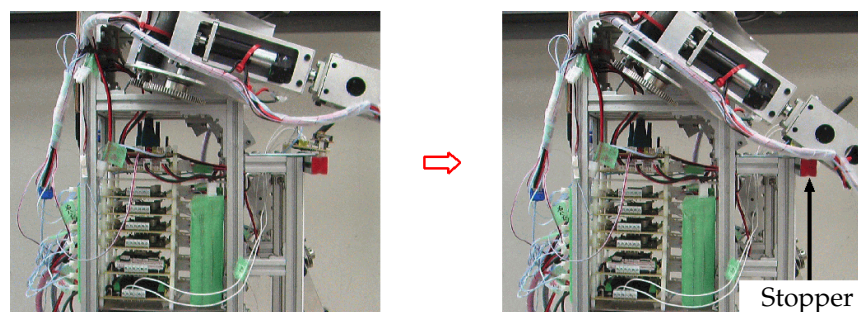**Figure 9.** Limit of manipulator rotation when the robot is being pulled.

Figure 10. Limit of manipulator rotation when the robot is being pushed.

The hand cart (PLA250-DB, Kanatsu, Chiyoda-ku, Tokyo, Japan) used in the present study is a commercially available hand cart (Figure 1, Table A2). The cart has a hand brake mechanism, which was remodeled to allow grasping (Figure 11). This hand brake mechanism has two shafts to allow holding, which are used to apply or release the cart brakes. When the robot hand grasps the hand brake system, the brake system is releases and the cart is able to move. When the robot hand releases the hand brake system, the brake is applied and the cart is not able to move. The robot and the cart are connected by the robot hands throughout the step-climbing process. Releasing or applying the hand brake is controlled by the angle of the forearm links of the manipulators because the hands have spaces between fingers (Figure 11). When the angle of forearm links is small, the brake is released, and when the angle of the forearm links is large, the brake is applied.

This cart also has a stopper that is composed of front and rear bars (Figure 12), and the stopper is mounted on the rear side. The stopper is not used for cart climbing, but rather for robot climbing (Figure 13). The details of the use of the cart stopper are presented in Section 3.

Figure 14 is a system configuration diagram. The robot has a notebook PC (OS: Windows Xp, msi U100, New Taipei City, Taiwan) on its body. The motors, encoders, and touch sensors were connected to motion controllers (MCDC3006-S, MCDC3003-S, Faulhaber Co. Ltd, Baden-Wuerttemberg, Germany).

These motion controllers were connected to the notebook PC of the robot. The motors were controlled via commands issued using the Motion Manager 4 software package (Faulhaber). The robot used a camera built into the PC, and moving images from the camera and the Motion Manager 4 operating window were displayed on the notebook PC mounted on the robot. The screen of this notebook PC used Real VNC software (version 4.1.2) and was transmitted as-is over an intranet to the display of a PC used by an operator at a different location. The operator of the robot was able to control the robot by operating Motion Manager 4 from their PC. Commands for Motion Manager 4 were issued using "JoyToKey" software. The keyboard commands, which were activated by pushing the buttons of a "Joypad" (PL-USGP12, Planex Communications Inc., Shibuya-ku, Tokyo, Japan), corresponded to manipulation of the controller to operate the robot. The controller is a commercially available game pad. The operator controls the robot by watching moving images returned from the camera on the robot. In the present study, the robot was operated at a constant speed (0.76 [km/h]).
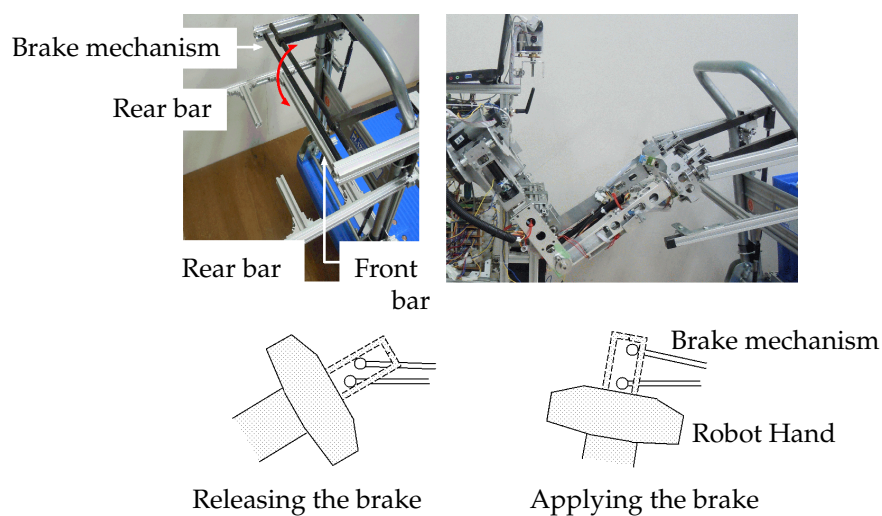
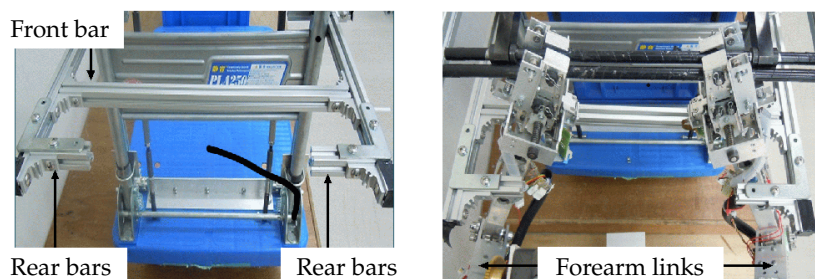**Figure 11.** Brake mechanism on the hand cart.

Figure 12. Stopper on the hand cart.
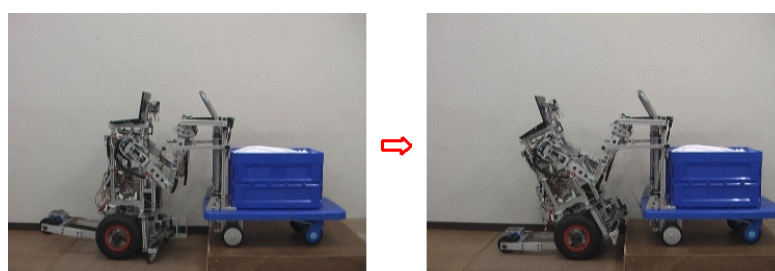
Figure 13. Robot lifting its front wheels.
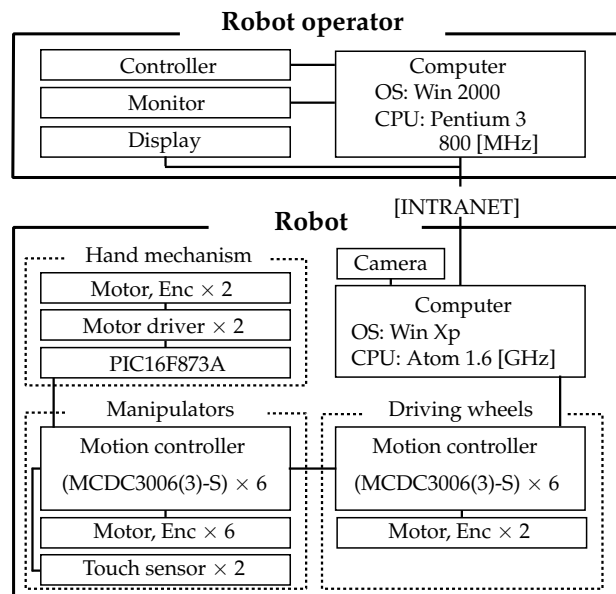
Figure 14. Block diagram of the robot system.

3. Process of Step Climbing

In the proposed step-climbing method, the hand cart first climbs a step, and then the robot climbs the step. In the present study, Stages 1 and 2, respectively, describe the processes by which the front and rear wheels of the cart ascend the step. Stage 3 describes the process by which the front wheels of the robot ascend the step. Stage 4 describes the processes in which the middle and rear wheels of the robot ascend the step. Numbers (1)–(16) in Figures 15 and 16 correspond to the states described below.

Figure 15. Step-climbing process of the hand cart.

stage 3   stage 4

(9)   (13)

(10)   (14)

(11)   (15)

(12)   (16)

Figure 16. Step-climbing process of the robot.

[Stage 1]

(1)   The upper links of manipulators are located behind the robot stopper (Figures 8 and 9). Joints 2, 4, and 6 are allowed to rotate passively until the ascent of the cart has been completed (Figure 7).
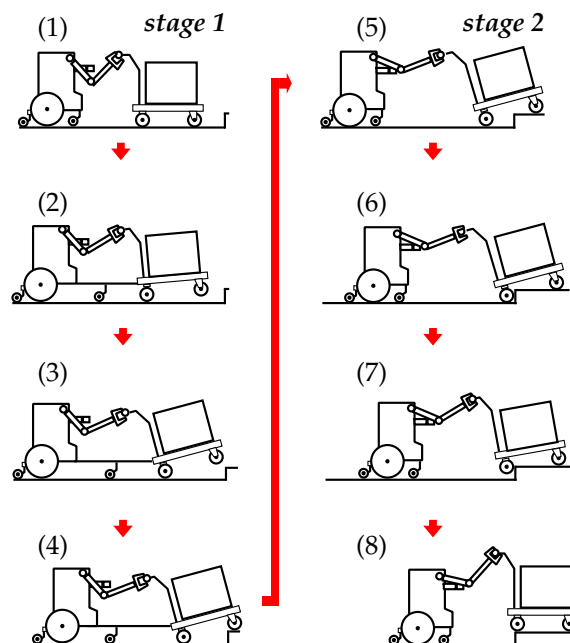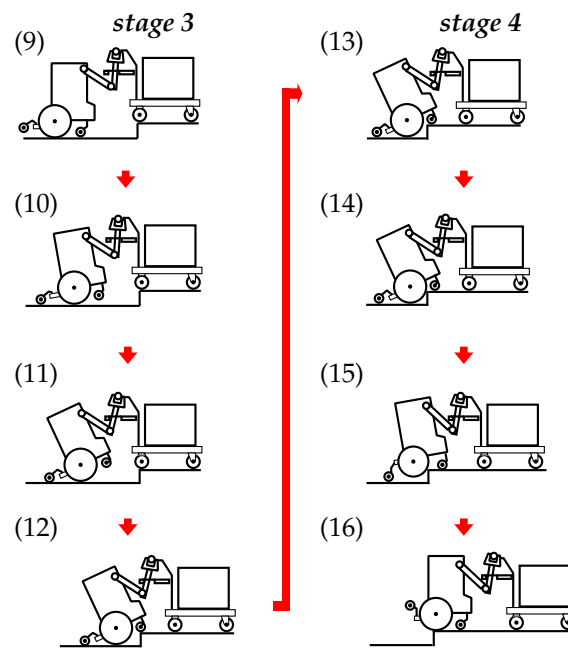
(2)   The robot stops and pushes against the rear bottom part of the cart using the robot front-wheel mechanism (Figure 6). The front wheels of the cart start to be lifted.

(3)   The robot continues to push the rear bottom part of the cart, and the cart tilt increases. The action for lifting the front wheels of the cart exerts forces on the manipulators, causing passive rotation about Joint 2. However, the upper arm link of the manipulator comes into contact with the robot stopper, limiting the extent of rotation (Figure 9).

(4)   The robot moves forward and the front wheels of the cart are positioned over the edge of the step. As the operator closes the robot front-wheel mechanism, the incline of the cart becomes small. The front wheels of the cart are located on the upper level of the step.

[Stage 2]

(5)   First, the sides of the robot manipulators are opened, and the upper links of the manipulators are located in front of the robot stopper (Figure 10). This limits the passive rotational travel of the manipulators when the robot is pushed. The robot then moves forward, pushing the cart from behind.

(6)   The rear wheels of the cart come into contact with the step.

(7)   The robot pushes the cart, and the rear wheels of the cart begin to climb the step. The robot imitates the operation of a human pushing an heavy object by limiting the passive rotation about the shoulder joints as the upper arms are pushed into the chest (Figure 4).

(8)   Once the rear wheels of the cart have reached the upper level of the step, the robot stops.

[Stage 3]

(9)   The sides of the robot are opened, and the two manipulators are inserted into the stopper of the cart (Figure 12). The rear wheels of the robot are folded upward (Figure 13). The robot moves forward and the manipulator forearm links come into contact with the stopper of the cart. The hand brake is applied. The cart maintains its position (Figure 11).

(10) The robot continues to push on the cart, and the front wheels of the robot are lifted (Figure 13).

(11)　When the location of the robot center of mass shifts behind the contact point between the robot middle wheels and the ground as the robot tilt increases, the robot begins to tip over backward. However, the robot is supported by the middle and rear wheels, and the rotational travel of the manipulators are stopped by the rear bars of cart's stopper. The brake of cart is then released (Figure 11).

(12)　The robot moves forward using the middle and rear wheels, and the front wheels of the robot are placed on the upper level of the step.

[Stage 4]

(13)　The robot drives and both vehicles move forward.

(14)　The middle wheels of the robot come into contact with the step.

(15)　The middle wheels of the robot continue to drive, and both vehicles continue to move forward. The rear-wheel mechanism of the robot is lowered and pushes up the robot body. The middle wheels of the robot start to climb the step.

(16)　The middle wheels of the robot are able to climb the step. After the middle wheels of the robot have reached the upper level of the step, the vehicles are stopped. The rear-wheel mechanism of the robot is then folded upward.

4. Theoretical Analysis

The proposed step-climbing method is sensitive to the relationship between the masses of the connected vehicles. In this section, we discuss the requirement for lifting the front wheels of the hand cart. The vehicles slowly climb a step and maintain their balance in the proposed method, which is analyzed by considering statics.

The basic coordinate system of the robot if denoted Σ_B, where contact point B between the robot middle (driving) wheels and the ground is the origin (Figure 17). In Stage 1, the inclination of the robot is zero ($\phi_0 = 0$). In Figure 3, the position vectors for these joints in system Σ_B are expressed as

$$^B\boldsymbol{p}_{2i} = [x_{2i} \ z_{2i}]^T \quad (i = 1-3), \tag{1}$$

where

$$^B\boldsymbol{p}_2 = [x_2 \ z_2]^T = [l_{LB} \ R_B + h_{LB}]^T \tag{2}$$

$$^B\boldsymbol{p}_4 = [x_4 \ z_4]^T = [l_{LB} + l_2\cos\phi_2 \ R_B + h_{LB} + l_2\sin\phi_2]^T \tag{3}$$

$$^B\boldsymbol{p}_6 = [x_6 \ z_6]^T = [l_{LB} + l_2\cos\phi_2 + l_{4c}\cos(\phi_2 + \phi_4) \ R_B + h_{LB} + l_2\sin\phi_2 + l_{4c}\sin(\phi_2 + \phi_4)]^T \tag{4}$$

In the same way, the position vectors for the contact points between the robot front and rear wheels and the ground are expressed as

$$^B\boldsymbol{p}_{fwb} = [WB_f \ 0]^T \tag{5}$$

and

$$^B\boldsymbol{p}_{rwB} = [-WB_r \ 0]^T \tag{6}$$

The position vectors for the contact points between the robot front-wheel mechanism and the rear of the hand cart are expressed as

$$^B\boldsymbol{p}_{fp} = [x_{pB} \ z_{pB}]^T. \tag{7}$$

The body of the robot, neglecting the manipulators, is Link 0 with mass m_0. If the centers of gravity of the robot body and each manipulator link (Links 2, 4, and 6) are denoted by

$$^B\boldsymbol{p}_{gj} = [x_{g2j} \ z_{g2j}]^T \quad (j = 0-3) \tag{8}$$

the vector of the driving force for the robot middle wheels and the resistance force from the ground surface is given by

$$f_m = [f_{1x} \quad f_{2z}]^T. \tag{9}$$

In addition, the resistance force vector at the robot front wheels is

$$f_{fwB} = [0 \quad f_{3z}]^T \tag{10}$$

and that at the rear wheels is

$$f_{rwB} = [f_{4x} \quad f_{5z}]^T. \tag{11}$$

The reaction force vector from the linked cart is

$$f_L = [f_l \cos(\phi_2 + \phi_4) \quad f_l \sin(\phi_2 + \phi_4)]^T \tag{12}$$

and the reaction force vector from the cart to the robot front-wheel mechanism is given by

$$f'_p = [-f_p \quad 0]^T. \tag{13}$$

The coordinate system fixed at the point of contact, A, between the cart rear wheels and the ground is given by Σ_A. The incline of the cart body with respect to the road surface is $\phi_2 + \phi_4 + \phi_6 = \phi_{246}$ (in Stages 1 and 2, the robot incline is zero $\phi_0 = 0$). In Σ_A, the center of gravity of the cart is located at

$$^A p_{GA} = [x_{GA} \quad z_{GA}]^T = [l_{rA} \cos \phi_{246} - h_{mA} \sin \phi_{246} \quad l_{rA} \sin \phi_{246} + h_{mA} \cos \phi_{246} + R_A]^T \tag{14}$$

and the push handle location (which is held by the robot hand), P_c (P_6), is

$$^A p_c = [x_c \quad z_c]^T = [-l_{LA} \cos \phi_{246} - h_{LA} \sin \phi_{246} \quad -l_{LA} \sin \phi_{246} + h_{LA} \cos \phi_{246} + R_A]^T. \tag{15}$$

The contact position between the body of cart and the robot front-wheel mechanism is located at

$$^A p_{fp} = [-l_{pA} \cos \phi_{246} - h_{pA} \sin \phi_{246} \quad R_A - l_{pA} \sin \phi_{246} + h_{pA} \cos \phi_{246}]. \tag{16}$$

The resistance force vector of the rear wheels of the cart from the ground surface is

$$f_{rwA} = [0 \quad f_{6z}]^T. \tag{17}$$

In addition, the reaction force from the linked robot is given by

$$f'_L = [-f_l \cos(\phi_2 + \phi_4) \quad -f_l \sin(\phi_2 + \phi_4)]^T. \tag{18}$$

The reaction force vector from the robot front-wheel mechanism to the cart is given by

$$f_p = [f_p \quad 0]^T. \tag{19}$$

In moving statically, the equilibrium of the robot along the x and z axes is given by the following equation:

$$f_{\Sigma B} + M_B g = 0, \tag{20}$$

where $f_{\Sigma B} \in R^2$ is the sum of forces on the robot due to the driving force and the resistances of the ground surface and the linked cart, and is given as

$$f_{\Sigma B} = [f_{1x} + f_{4x} + f_l \cos(\phi_2 + \phi_4) - f_p \quad f_{2z} + f_{3z} + f_{5z} + f_l \sin(\phi_2 + \phi_4)]^T \tag{21}$$

and

$$g = [0 \ -g]^T \tag{22}$$

is the gravitational acceleration vector.

The following equation is obtained from the equilibrium of moments about the point of contact between the robot middle wheels and the ground:

$$^B\boldsymbol{p}_{GB} \times M_B\boldsymbol{g} + {}^B\boldsymbol{p}_4 \times \boldsymbol{f}_L + {}^B\boldsymbol{p}_{fwB} \times \boldsymbol{f}_{fwB} + {}^B\boldsymbol{p}_{rwB} \times \boldsymbol{f}_{rwB} + {}^B\boldsymbol{p}_{fp} \times \boldsymbol{f}'_p = 0. \tag{23}$$

Equation (24) is obtained from Equation (23), as follows:

$$-x_{GB} \cdot M_B g + x_4 \cdot f_l \sin(\phi_2 + \phi_4) - z_4 \cdot f_l \cos(\phi_2 + \phi_4) + WB_f \cdot f_{3z} - WB_r \cdot f_{5z} + z_{pB} \cdot f_p = 0. \tag{24}$$

Summing the total forces on the hand cart exerted by the ground surface and the linked robot for $f_{\Sigma A} \in \boldsymbol{R}^2$, we find that

$$\boldsymbol{f}_{\Sigma A} = [f_p - f_l \cos(\phi_2 + \phi_4) \quad f_{6z} - f_l \sin(\phi_2 + \phi_4)]^T \tag{25}$$

When the linked vehicles move together in static equilibrium, the equilibrium for both the x and z axes yields

$$\boldsymbol{f}_{\Sigma A} + M_A\boldsymbol{g} = 0, \tag{26}$$

whereas the equilibrium of moments about the point of contact between the rear wheels of the hand cart and the ground yields

$$^A\boldsymbol{p}_{GA} \times M_A\boldsymbol{g} + {}^A\boldsymbol{p}_c \times \boldsymbol{f}'_L + {}^A\boldsymbol{p}_{fp} \times \boldsymbol{f}_p = 0. \tag{27}$$

We obtain the following equation from Equation (26):

$$f_p = f_l \cos(\phi_2 + \phi_4). \tag{28}$$

The requirement for lifting the front wheels of the hand cart is obtained from Equation (27) as follows:

$$-x_{GA} \cdot M_A g - x_c \cdot f_l \sin(\phi_2 + \phi_4) + z_c \cdot f_l \cos(\phi_2 + \phi_4) - z_{pA} \cdot f_p > 0. \tag{29}$$

Substituting Equation (28) for Equation (29), we obtain

$$x_{GA} \cdot M_A g + f_l \cdot \{x_c \sin(\phi_2 + \phi_4) + (z_{pA} - z_c)\cos(\phi_2 + \phi_4)\} < 0, \tag{30}$$

and substituting Equation (28) for Equation (24), we obtain

$$f_l = \frac{x_{GB} \cdot M_B g - WB_f \cdot f_{3z} - WB_r \cdot f_{5z}}{x_4 \sin(\phi_2 + \phi_4) + (z_{pB} - z_4)\cos(\phi_2 + \phi_4)}. \tag{31}$$

We assume the most difficult situation is to lift the cart's front wheels, in which the robot does not use its rear wheels (Figure 17, $f_{5z} = 0$) and the robot is pushed by the reaction force from the hand cart and the normal force of the front wheels of the robot ($f_{3z} = 0$). In this case, by substituting Equation (31) for Equation (30), we obtain the requirement for lifting the front wheels of the hand cart as follows:

$$\frac{M_A}{M_B} < \frac{(z_{pA} - z_c)\cos(\phi_2 + \phi_4) + x_c \sin(\phi_2 + \phi_4)}{(z_4 - z_{pB})\cos(\phi_2 + \phi_4) - x_4 \sin(\phi_2 + \phi_4)} \cdot \frac{x_{GB}}{x_{GA}}. \tag{32}$$

When Equation (32) is satisfied, the front wheels of the hand cart can be lifted by the robot. Tables A1 and A2 indicate that the robot is able to lift the hand cart in theory. In the next section, we present the results of the experiment.
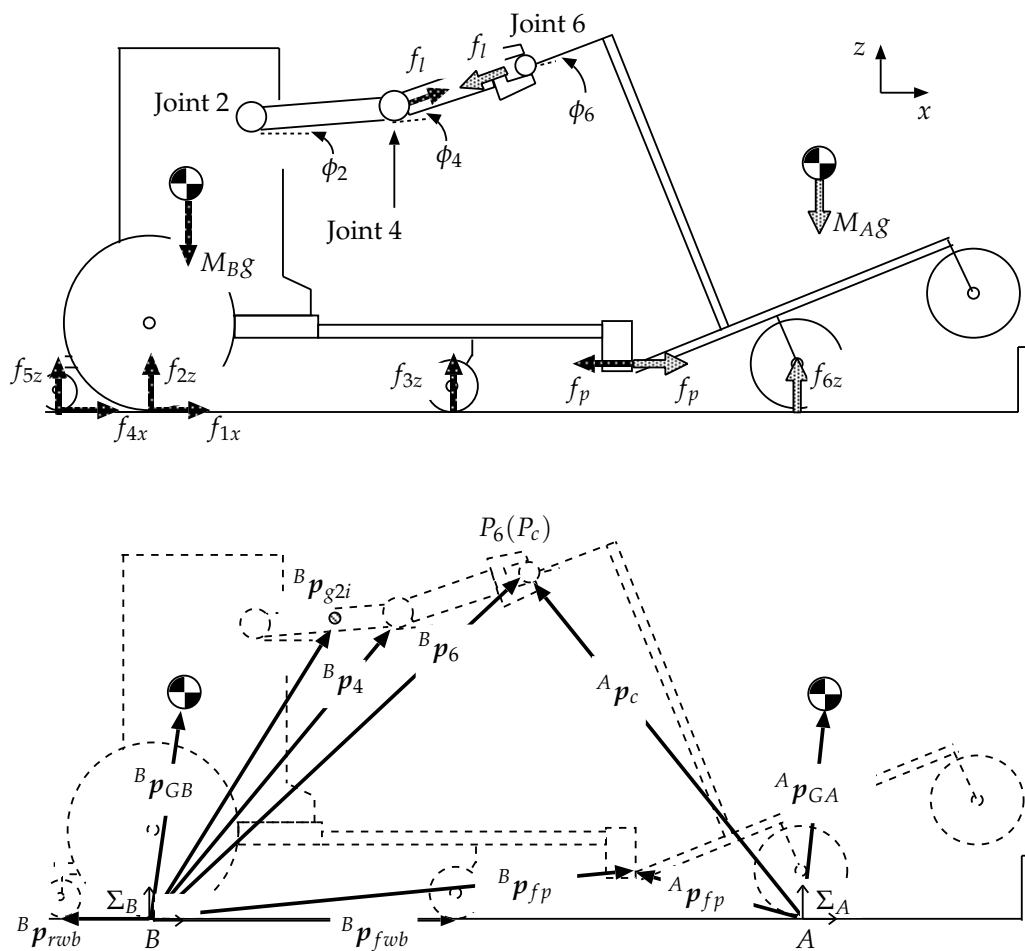
Figure 17. Model showing lifting of the front wheels of the hand cart.

5. Experiment

Experiments were carried out under an environment with a step of 120 mm in height, and the mass of the hand cart was 75 kg (body of the cart: 25 kg, baggage: 50 kg).

The speed of the robot was constant (0.76 km/h), and the friction coefficient between the tires and the road surface was $\mu = 0.72$ (Figure 18). The robot and the hand cart were located on one floor of the National Institute of Technology of Toyama College, and the operator of the robot (adult male) was located on another floor. The robot operator performed his task over an intranet while observing the video from the camera on the robot.

In Stage 1, the robot operator was able to lift the front wheels of the cart and position them on the step by watching video captured by the robot camera. After climbing of the front wheels of the hand cart, the operator was able to change the manipulators' upper link positions from behind the robot stopper to in front of the robot stopper (Section 3, Figures 9 and 10). However, the operator needed approximately 90 s to change these positions. In the present paper, the robot and the hand cart are connected, and the trajectories of these vehicles are limited. Teleoperation of the robot using a game pad controller when the positions of the manipulators change was difficult, indicating that the robot should have an autonomous system for positioning the manipulators.

In Stage 2, it was possible for the rear wheels of the hand cart to climb the step with ease.

In Stages 3 and 4, the step-climbing process of the robot was performed. Although the robot was able to climb the step, it was difficult to operate the robot while viewing video captured by the camera on the robot because the robot is inclined during Stages 3 and 4 and the operator was not able to view the state of the vehicles. Another experiment was carried out using an additional camera on the chest

of the robot (same operator), and the operability of robot was improved. The climbing task was also performed successfully by another operator (adult male).

The results of these experiments clarified that the proposed step-climbing method is useful and can be improved by adding an autonomous system to change the manipulator position.
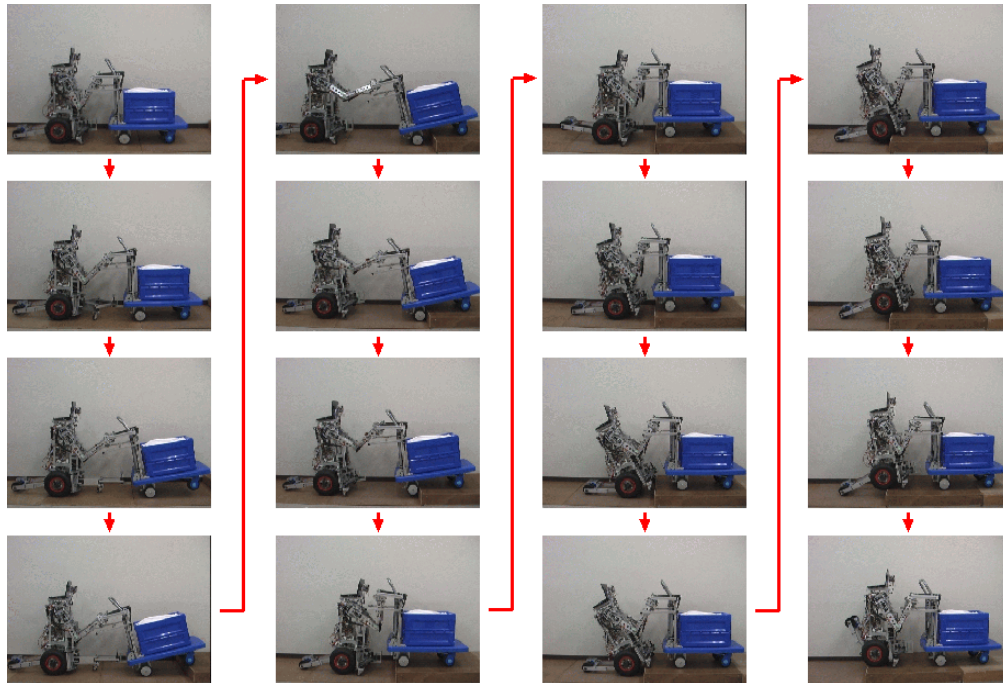

Figure 18. Step-climbing experiment using the robot and the hand cart.

6. Conclusions

The present paper describes the proposed step-climbing method of the hand cart using a partner robot that imitates human motion when operating a hand cart. The system, which consists of a mobile robot and a hand cart, was constructed. Numerical calculations clarified the requirements of masses and centers of gravity for both vehicles to lift the cart. Experiments were carried out incorporating teleoperation of the robot over an intranet, in which the robot operator controlled the robot while viewing video captured by the robot camera.

The results of the experiment are listed below.

(1)　The teleoperated robot and the hand cart are able to climb a step using the proposed method.
(2)　The operator requires some time (approximately 90 s) to change the position of the manipulators (after Stage 1). Both vehicles have individually driven wheels and are connected, and thus the trajectories of the vehicles are limited. Moreover, the teleoperated robot was controlled using a game pad, making operation of the robot difficult and indicating that system for changing the positions of the manipulators should be autonomous.
(3)　The camera on the robot cannot capture the entire situation of the vehicles. However, the additional camera on the robot chest was able to improve operability. The climbing task was also performed successfully by another operator.

Nevertheless, a mobile robot with manipulators can make a heavy hand cart climb a step. The proposed method is relatively simple and can be applied to other partner robots, thereby improving their abilities.

In the future, we intend to improve the maneuverability of the proposed step-climbing method and evaluate the operability of the system. We are going to construct an autonomous system for positioning the manipulators.

Appendix A

Table A1. Specifications of the robot.

Overall length	230–800 mm
Overall height	747 mm
Radius of front wheels (r_{Bf})	25 mm
Radius of center wheels (R_B)	145 mm
Radius of rear wheels (r_{Br})	19 mm
Length of the front-wheel mechanism (l_{pB})	250–750 mm
Height of the front-wheel mechanism (h_{pB})	250–70 mm (when the incline of the cart is 0)
Wheelbase (WB_f)	190–440 mm
Wheelbase (WB_r)	270 mm
Mass position from the rear axis (l_{rB})	93 mm
Height of the mass from the rear axis (h_{mB})	286 mm
Position of Joint 2 from the rear axis (l_{LB})	90 mm
Height of Joint 2 from the rear axis (h_{LB})	532 mm
Mass of the robot's body	56.2 kg
Mass of Link 2 (from Joint 2 to Joint 4)	2.55 × 2 kg
Mass of Link 4 (form Joint 4 to the human hand)	0.8 × 2 kg
Length of Link 2 (l_2)	330 mm
Length of Link 4 (l_4)	300 mm
Length of the hand (l_6)	105 mm
Length from Joint 4 to the connecting position (l_{4c})	370 mm
Mass position of Link 2 (L_2)	67 mm
Mass position of Link 4 (L_4)	169 mm
Mass position of Link 6 (L_6)	35 mm

Table A2. Specifications of the hand cart.

Overall length	1020 mm
Overall height	900 mm
Radius of the front and rear wheels (R_A)	65 mm
Wheelbase (l_A)	470 mm
Connecting height (h_{LA})	695 mm
Connecting position (l_{LA})	270 mm
Stopper position (front bar) from the axis of the rear wheels	210 mm
Stopper position (rear bars) from the axis of the rear wheels	360 mm
Stopper Height from the axis of the rear wheels	500 mm
Length of contact position (l_{pA})	160 mm
Height of contact position (h_{pA})	150 mm
Mass position (l_{rA})	235 mm
Mass height (h_{mA})	350 mm
Mass (M_A)	75 kg

References

1. Onozato, T.; Tamura, H.; Kambayashi, Y.; Katayama, S. A Control System for the Robot Shopping Cart. In Proceedings of the 2010 ERAST International Congress on Computer Applications and Computational Science, Singapore, 4–6 December 2010; pp. 907–910.

2. Sales, J.; Mart, J.V.; Marn, R.; Cervera, E.; Sanz, P.J. CompaRob: The Shopping Cart Assistance Robot. *Int. J. Distrib. Sens. Netw.* **2015**, 1–15. [CrossRef]

3. Lee, H.; Lee, G.; Kwon, C.; Noguchi, N.; Chong, N.Y. Swithched Observer Based Impedance Control for an Assistive Robotic Cart unbder Unknown Parameters. In Proceedings of the IEEE RO-MAN: The 21st IEEE International Symposium on Robot and Human Interactive Communication, Paris, France, 9–13 September 2012; pp. 101–106.

4. Takahashi, T.; Suzuki, T.; Shitamoto, H.; Moriguchi, M.; Yoshida, K. Developing a mobile robot for transport applications in the hospital domain. *Robot. Auton. Syst.* **2010**, *58*, 889–899. [CrossRef]

5. Scholz, J.; Chitta, S.; Marthi, B.; Likhachev, M. Cart pushing with a mobile manipulation system: Towards navigation with moveable objects. In Proceedings of the 2011 IEEE International Conference on Robotics and Automation, Shanghai, China, 9–13 May 2011; pp. 6115–6120.

6. Iwamura, Y.; Shiomi, M.; Kanda, T.; Ishiguro, H.; Hagita, N. Do elderly people prefer a conversational humanoid as a shopping assistant partner in supermarkets? In Proceedings of the 6th International Conference on Human-Robot Interaction, Lausanne, Switzerland, 6–9 March 2011; pp. 449–456.

7. Ohno, N.; Hasegawa, T. Controller of Mobile Robot. U.S. Patent US8340823 B2, 25 December 2012.

8. Nozawa, S.; Maki, T.; Kojima, M.; Kanzaki, S.; Okada, K.; Inaba, M. Wheelchair support by a humanoid through integrating environment recognition, whole-body control and human-interface behind the user. In Proceedings of the 2008 IEEE/RSJ International Conference on Intelligent Robots and Systems, Nice, France, 22–26 Septmber 2008; pp. 1558–1563.

9. Nakajima, S.; Nakano, S.; Takahashi, T. Free gait algorithm with two returning legs of a leg-wheel robot. *J. Robot. Mechatron.* **2008**, *20*, 661–668. [CrossRef]

10. Kumar, V.; Krovi, V. Optimal Traction Control In A Wheelchair With legs And Wheels. In Proceedings of the 4th National Applied Mechanisms and Robotics Conference, Cincinnati, OH, USA, 10–13 December 1995.

11. Gonzalez, A.; Ottaviano, E.; Ceccarelli, M. On the Kinematic Functionality of s Four-bar Based Mechanism for Guiding Wheels in Climbing Steps and Obstacles. *Mech. Mach. Theory* **2009**, *44*, 1507–1523. [CrossRef]

12. Independence Technology, L.L.C., iBOT. Available online: http://www.hizook.com/blog/2009/02/11/ibot-discontinued-unfortunate-disabled-perhaps-budding-robotics-opportunity (accessed on 11 February 2009).

13. Asama, H.; Sato, M.; Goto, N.; Kaetsu, H.; Matsumoto, A.; Endo, I. Mutual transportation of cooperative mobile robots using forklift mechanisms. In Proceedings of the 1996 IEEE International Conference on Robotics and Automation, Minneapolis, MN, USA, 22–28 April 1996.

14. Ikeda, H. Step climbing strategy for a wheelchair. In *Advances in Intelligent Systems: Reviews*; Reviews Book Series; Yurish, S., Ed.; IFSA Publishing, S.L.: Barcelona, Spain, 2017; Volume 1, Chapter 10, pp. 249–288.

15. Ikeda, H.; Hashimoto, K.; Murayama, D.; Yamazaki, R.; Nakano, E. Collision avoidance between a wheelchair front wheels and a step wall during step climbing using a care robot. *Adv. Sci. Technol. Eng. Syst. J.* **2017**, *2*, 732–740. [CrossRef]

16. Ikeda, H. Establishment of step climbing technology for a heavy carrier using a robot which is driven by low power motors. *Rep. Matsuda Found.* **2014**, *26*, 87–94. (In Japanese)